Encoding-based brain-computer interface controlled by non-motor area of rat brain

LANG YiRan[*], DU Ping & SHIN Hyung-Cheul

Department of Physiology, College of Medicine, Hallym University, Chuncheon 200-702, Republic of Korea

As the needs of disabled patients are increasingly recognized in society, researchers have begun to use single neuron activity to construct brain-computer interfaces (BCI), designed to facilitate the daily lives of individuals with physical disabilities. BCI systems typically allow users to control computer programs or external devices via signals produced in the motor or pre-motor areas of the brain, rather than producing actual motor movements. However, impairments in these brain areas can hinder the application of BCI. The current paper demonstrates the feasibility of a one-dimensional (1D) machine controlled by rat prefrontal cortex (PFC) neurons using an encoding method. In this novel system, rats are able to quench thirst by varying neuronal firing rate in the PFC to manipulate a water dish that can rotate in 1D. The results revealed that control commands generated by an appropriate firing frequency in rat PFC exhibited performance improvements with practice, indicated by increasing water-drinking duration and frequency. These results demonstrated that it is possible for rats to understand an encoding-based BCI system and control a 1D machine using PFC activity to obtain reward.

brain-computer interface, prefrontal cortex, rat, one-dimensional, single neuron recording

Brain-computer interfaces (BCI) enable patients with motor-related disabilities [1] and healthy individuals to manipulate prostheses and computer programs directly via their brain activity, with invasive [2,3] or non-invasive systems [4–6]. Recently, several groups have investigated the possibility of cortically-controlled neural prostheses [7–15]. Neuronal activity in the premotor, primary motor and posterior parietal cortical areas of non-human primates has been successfully used to control motor tasks [16] in BCI systems. Studies have shown that primates can learn to reach and grasp virtual objects by controlling a robot arm through a closed-loop brain-machine interface using mathematical modeling to extract several motor parameters from the electrical activity of frontoparietal neuronal ensembles [17]. In such a system, monkey primary motor neurons are decoded into a signal that can move a computer cursor to a new position in two-dimensional space [18]. These methods transform neuronal population signals in the motor areas into real-time movements of prosthetic devices. Unfortunately, this type of motor information cannot be obtained in patients with disorders affecting motor-related brain areas. It is well established that the prefrontal cortex (PFC) is associated with behavioral flexibility, working memory, planning, spatial navigation, and goal-directed behavior [19, 20]. Despite the important functions of the PFC, it has never been utilized in BCI systems.

Increased understanding of the way in which the brain represents movement would facilitate the design of appropriate decoding algorithms, which form the basis of current BCI research. Nonetheless, we hypothesize that it is not necessary to fully decode neural signals. Simple models and

*Corresponding author (email: langyiran@sina.com)

encoding algorithms may be sufficient for the neural control of devices, since the brain is a complex learning system that can learn new arbitrary tasks with appropriate training. In the current study, we developed a relatively simple algorithm for rats to control a BCI system using neuronal activity in the PFC.

1 Materials and methods

1.1 Implantation surgery and electrophysiology

Experiments were approved by the Hallym University Animal Care and Use Committee. Sprague-Dawley rats (230–280 g) were used in this study, obtained from the Experimental Animal Center of Orient Bio Co., Seongnam-si, Korea. The environment of the breeding room was maintained at $(23\pm2)°C$ and relative humidity was $50\%\pm10\%$. Artificial lighting was used to light the room for 12 h per day. For surgery, rats were anesthetized with ketamine (i.m., Yuhan, Seoul, Korea; 100 mg kg^{-1}) and xylazine (Bayer Korea, Seoul, Korea; 5 mg kg^{-1}). A relatively large craniotomy (2–3 mm in diameter) was made bilaterally over the PFC. The PFC region (2.7 mm anterior to bregma, 0.5–1.0 mm lateral from midline, 1.8–2.0 mm ventral to the dorsal surface of the brain surface) of the left and right PFC was identified according to a previously published rat brain map [21], and one or two multi-wire recording electrodes (tungsten microwire, A-M systems, USA; 40 μm in diameter, teflon-coated) were lowered into the cortex, targeting layer IV of the PFC (Figure 5E) with a hydraulic device (Narishige, Tokyo, Japan). The custom-made 8-channel electrode array (2×4) consisted of two bundles of four microwires. Each bundle was separated by approximately 1 mm and the interval between adjacent microwires was approximately 50 μm. After verification of single neuron activity, the base of the electrode bundles was covered with gel-foam and cemented to the pre-screwed anchors with dental resin. The ground wire was attached to one of the screws penetrating the skull, 3 mm away from electrode bundles.

After surgery, a recovery period at least one week was allowed before experimentation. Forty-eight hours prior to the experiment, rats were deprived of water to increase thirst. Each rat was placed into the experimental cage and the rat was implanted with the electrode connector to check for the presence of neurons using a data acquisition system (MAP, Plexon Inc., Dallas TX, USA) for online multi-channel spike sorting and unit recording. The MAP system recorded up to 64 continuous analog signals at 40 kHz using National Instruments Data Acquisition (NI DAQ, National Instruments Co., Texas, USA) devices. A pre-amplifier delivered improved signal-to-noise (10 times of gain) and jumperable analog low-cut filter selection to a computer. For spike recording, low-cut of bandpass was 150 Hz and high-cut was 3 kHz. The signals were improved digitally by applying 20000 times the gain with the computer system.

The raw signals were overlapped every 800 μs with a window discriminator (Figure 1A), and sorted on the basis of amplitude and peak-to-peak distance. Power spectral density analysis was used to rule out the environmental noise (for example, 30 Hz power consumption). Signals with a signal-to-noise ratio lower than 3:1 were discarded. Autocorrelograms were examined off-line after sorting single cell signals. If no clear refractory period (1–2 ms) was detected in the autocorrelogram, additional feature combinations were examined to subdivide the cluster further until a clear refractory period was presented in the autocorrelogram [22]. Templates of the units were prepared and saved separately for each rat for later use.

1.2 Algorithm

Among simultaneously recorded units, two (N1 and N2) were selected and their activities were converted in every 200 ms to commands through a triple threshold comparator algorithm (Figure 1B). Pre-processing was applied to 40 s of data to calculate the mean firing rate and standard deviation (SD) under normal resting conditions. The activity of N1 and N2 neurons was measured to serve as baseline and converted to four activity ranges around the mean firing rates ($M\pm(0.5\times SD)$). The four firing ranges ($\geqslant(M+0.5\times SD)+1$, $M\sim M+0.5\times SD$, $M-0.5\times SD\sim M-1$, $\leqslant(M-0.5\times SD)-1$) of N1 and N2 were normalized by assigning four command values for clockwise (CW; 3, 2, 1, 0) and counter-clockwise (CCW; 0, −1, −2, −3) rotation of water dish. N1 was responsible for CW and N2 was responsible for CCW movement. Machine control commands were generated by the values resulting from the addition of CW and CCW commands. The i80196 microprocessor thus received seven types of commands (3, 2, and 1 for CW; −1, −2, and −3 steps of rotation for CCW; and 0 for STOP) from the control PC, and executed them accordingly. One step of rotation in any direction turned the wheel exactly 14.5°, two steps turned it 21.5°, and three steps turned it 28.5°, respectively. When no turn (STOP) command was received, the stepper motor's magnetic force strongly grabbed the axis of rotation, so it was impossible to rotate the wheel by external force from animals. A 'FLUSHING' command generates a compelled rotation of the wheel when the STOP command was continuously transmitted for 5 s. This was implemented to disable any long periods of water drinking, which could result in the early termination of the session. The FLUSHING command rotated the wheel in the opposite direction of the previous rotation, by the number of degrees corresponding to three steps.

1.3 Experimental procedures

In the animal chamber of the BCI system, a rat was placed

in front of a horizontally rotating cylinder (10.0 cm in diameter) with circular dish (7 cm in diameter) containing water in the black painted quadrant on it (Figure 1A). The height of the circular dish was the same as that of the floor of the chamber. Drinking was made possible by maintaining the water dish in front of the rat. Three narrow flat steel platforms (4 cm long, 5 mm wide) were placed at the floor edge to prevent the rats grasping the dish with their forepaws. An experimental session would be initiated only if a rat showed continuous (more than 40 s without distraction) water-seeking behavior three times within 3 min.

A session of machine control trials (T) for 6 min was followed by a 6 min rest session (REST) in which water dish was blocked by a white paper wall. This sequence of wheel control and rest period was repeated 3–6 times until the rat showed no interest in drinking. After the last trial, rats were allowed access to food pellets (free food period, FF; Figure 3C and D, Figure 4D and E) but water access was blocked. Water was then offered freely for 6 min (free water period, FW; Figure 3C and D, Figure 4D and E) respectively. The actual wheel rotations were switched off but unit recordings and command generation were recorded during FF and FW. A video camera positioned 40 cm above the mechanical apparatus recorded all experimental sessions to monitor the rats' behavior. AVI format files were recorded at 30 Hz and compressed using Microsoft MPEG-4 video codec V2 (compression rate of 100%). Synchronization between the data acquisition system and video recordings was achieved using a light emitting diode that lit up at the start of the neuronal spike recording. The timings of the beginning and the end of water drinking were manually marked by frame-by-frame reviews of the video recordings by the investigators, with an accuracy of ±1 video frame. These timings were input into the computer to correlate neuronal activity during the water drinking (WD) and non-WD periods.

1.4   Data analysis

Statistical analysis was carried out using Graphpad Prism 4.0 (GraphPad Software, Inc., USA) and InStat 3.05 (GraphPad Software, Inc., USA). One way repeated-measures of analysis of variance (ANOVA) was used to test the statistical significance of differences within groups of individual units between different behavioral conditions. All pair-wise multiple comparison procedures (Student-Newman-Keuls method) were also applied to isolate the group or groups that differed significantly from the others. In every case, *P*-values less than 0.05 were considered to indicate statistical significance.

Firing frequency of neuronal signals was binned every 10 ms (number of spikes in every 10 ms was converted into count s^{-1}) and no smoothing or overlapping was applied after calculation.

1.5   Histological identification

For the histological analysis, animals were anesthetized with sodium pentobarbital (30 mg kg^{-1}, i.p.) and perfused transcardially with 0.1 mol L^{-1} phosphate-buffered saline (PBS, pH 7.4) followed by 4% paraformaldehyde in 0.1 mol L^{-1} phosphate-buffer (PB, pH 7.4). Brains were removed and postfixed in the same fixative for 6 h. The brain tissues were cryoprotected by infiltration with 30% sucrose overnight. Thereafter, frozen tissues were serially sectioned with a cryostat (Leica, Germany) into 30-μm coronal sections, then collected into six-well plates containing PBS. Cresyl violet staining was conducted to obtain a clear view of target area. The sections were mounted on gelatin coated microscopic slides. Cresyl violet (CV) acetate (Sigma, MO) was dissolved at 1.0% (w/v) in distilled water, and glacial acetic acid was added to t he solution. Before and after staining for 2 min at room temperature, the sections were washed twice in distilled water, dehydrated by placing successively for 2 h in 50%, 70%, 80%, 90%, 95%, 100% ethanol baths at room temperature, and finally mounted with Canada balsam (Kanto, Tokyo, Japan; Figure 5E) [23].

2   Results

In total, we analyzed experimental results from 56 trials, 56 rest sessions, as well as FW, FF, and FAR sessions, in 16 rats. The attention of rats was measured by focusing time when the dish was located in front of animals at the minimum distance for the dish to be out of their reach; this distance differed according to the reaching ability of animals. The duration of recording summed to a total of more than 600 min. Rats were allowed 30 min to adapt to the environment before the experiment began.

Figures 1 and 2 show an example of machine control. Fourteen single units were simultaneously recorded, and units 7b and 7d, isolated using a microwire, were used for machine control (Figure 1A and B). As in Chapin's (1999) paradigm [24], we used percentage of success in obtaining water reward as a measure of efficiency. Overall wheel rotations in a trial comprise repetitions of two periods: the WD and no-WD (NWD) periods. Video analyses revealed clear increases of WD frequency and total WD duration as trials were repeated from T1 to T5 (Figure 1C). The total WD duration in the first time-period (T1) was less than 1% of 6 min, while that at T6 was more than 26%. This performance elevation was mainly due to increases in WD frequency ((r)=0.9950), since averaged WD durations (in s, T1: 1, T2: 1.57±0.26, T3: 2.24±0.38, T4: 2.70±0.30, T5: 3.12±0.38) were not significantly different among five trials (*P*=0.0673, Kruskal-Wallis Test). WD events occurred intermittently at T2 and T3, but were spread over the entire 6 min period of T5 (Figure 1D).

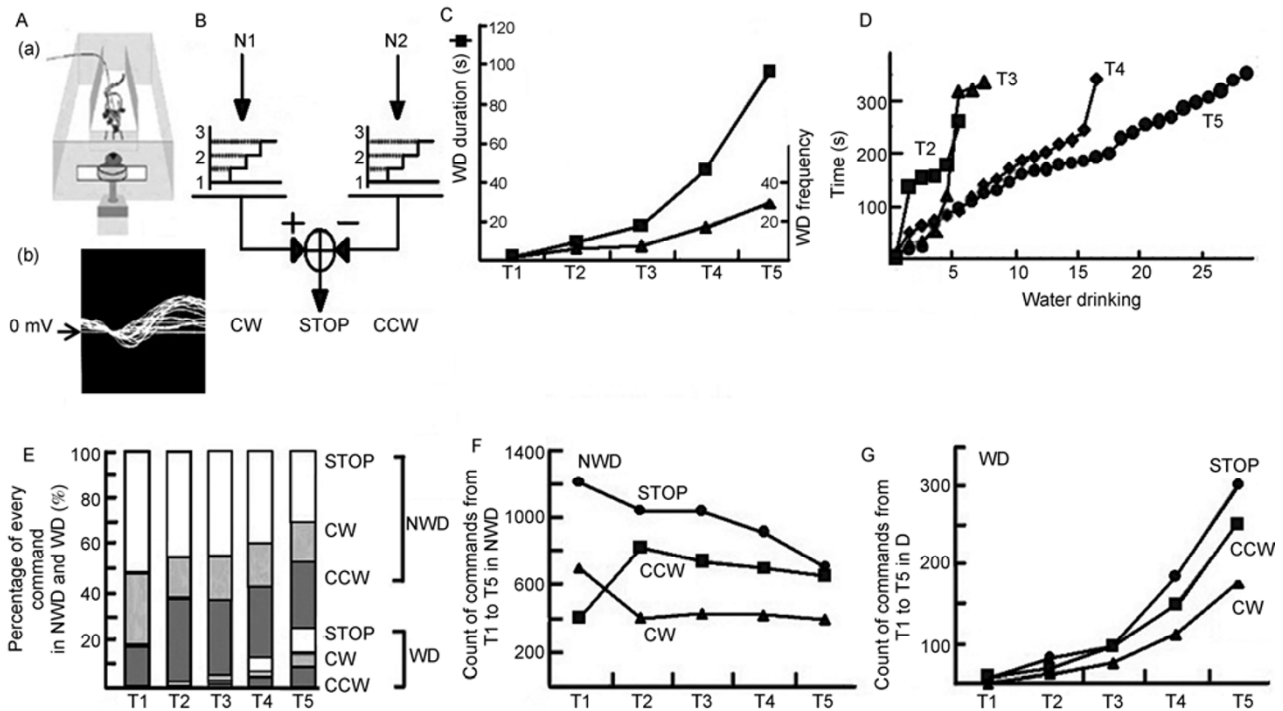Wheel rotations were controlled by CW, CCW, and

Figure 1　A, (a) Setup of 1-D system. A computer interface in which rats could freely move in a chamber, facing a water containing dish in the same plane of chamber. (b) Sample signals overlapped in a window discriminator. B, Triple-threshold algorithm for generating rotating command after comparing activities of two neurons. N1, neuron 1; N2, neuron 2. CW, clockwise; CCW, counterclockwise. C, WD duration and WD frequency changed across trials. D, Accumulative graph showing WD in every trial. E, Proportional movement-command distribution during NWD and WD. F, Count of movement-command changes over trials during NWD. G, Count of movement-command changes over trials during WD.

STOP commands. The STOP command constituted 52.17% of all commands generated during T1, but this ratio was reduced to 41.24% in T5 (Figure 1E). Although STOP commands during NWD period from T1 to T5 were gradually decreased (Figure 1F), those during the WD period were gradually increased as trials progressed (Figure 1G). STOP commands in the NWD period varied inversely to the frequency of WD from T1 to T5 ((r)=−0.9804). During NWD periods from T1 to T5, changes in the frequencies of CW and CCW commands were observed in opposite directions ((r)=−0.9147). CW rotations were common at T1, but CCW rotations were dominant over CW rotations from T2 to T5 (Figure 1F). During WD periods, the frequency of CW, CCW, and STOP commands all increased (Figure 1G), and changes in the frequencies of these commands were strongly related ((r)>0.99) to changes of both WD frequency and total WD duration.

　　Neural activity of both 7b and 7d prior to command generation were reflected the operation of the triple-step threshold comparator algorithm (Figure 1B). 7b and 7d were set to encode CW and CCW commands, respectively. Triple-step thresholds for unit 7b were set to 29, 27, 25 in Hz (CW threshold values: above 29: 3, 27–28: 2, 25–26: 1, below 25: 0) and those of 7d were to 27, 23, 19, in Hz (CCW threshold values: above 27: 3, 23–26: 2, 19–22: 1, below 19: 0). In the 200 ms period prior to either CW or CCW command generation, both neurons behaved antago-

nistically (Figure 2A and B). For the T5 WD period, neuron 7b exhibited elevated activity ((35.95±1.72) Hz), generating three steps of CW rotation (i.e., threshold value 3 for CW), whereas neuron 7d exhibited suppressed activity ((18.69±1.05) Hz, i.e., threshold value 0 for CCW) prior to CW commands. In the generation of CCW commands, neuron 7d exhibited heightened activity ((33.23±1.16) Hz, i.e., threshold value 3 for CCW), while unit 7b exhibited a lowered firing rate ((17.91±1.04) Hz, i.e., threshold value 0 for CW). STOP commands were generated when activity rates between both neurons were not significantly different (7b ((23.68±0.72) Hz) vs. 7d ((21.34±0.57) Hz): *P*>0.05; Figure 2C). However, corresponding threshold values for 7b and 7d were CW 0 and CCW 1, respectively. This appeared to contradict to the triple-threshold comparator algorithm to generate STOP commands. The finding that 7d's activities were not significantly different (*P*>0.05) for the generation of CCW 1 and CCW 0 suggests that STOP commands mainly occurred when both neurons' activities were at the threshold value 0. Neuron 7b exhibited significantly different firing rates for each of three commands (CW vs. CCW, *P*<0.001; CCW vs. STOP, *P*<0.01; CW vs. STOP, *P*<0.001) and threshold values segregated into two levels, fluctuating mainly between CW 3 and CW 0. Neuron 7d exhibited substantially different activity between CW and CCW rotations (*P*<0.001) and between CCW and STOP commands (*P*<0.001). Threshold values varied among CCW 3, CCW 1
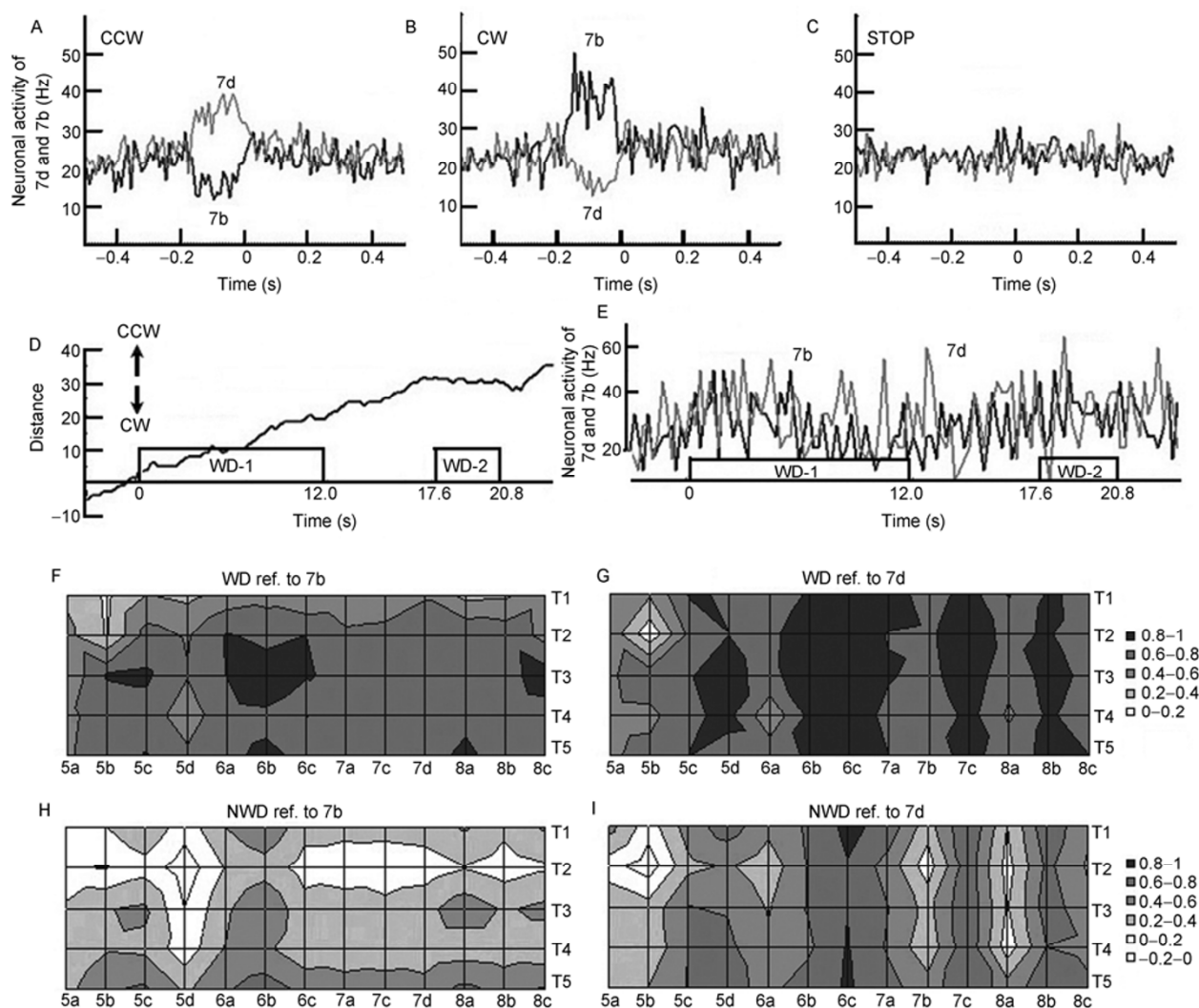
Figure 2   A, Opposite neuronal activity change producing CCW command. B, Opposite neuronal activity change producing CW command. C, Neuronal activity generating a STOP command. D, The distance of the dish within two WD durations. E, Two neuronal activities occurring in the same period. F–I, Correlations between other cells and cells 7b and 7d from T1 to T5.

and/or 0. Thus, CCWs tended to involve three-step movements, while CWs tended to involve either three- or two-step movements. This ensured the dominant generation of CCW over CW. Similar activity ranges of neuron 7d also provided the flexibility to generate either CW 2 or STOP commands. Although for background periods of 301 to 500 ms prior to and 500 ms post to CW command generation neurons 7b ((24.35±0.45) Hz) and 7d ((24.21±0.42) Hz) showed similar firing rates, 7b exhibited significantly lower activities than 7d (7b, (22.20±0.40) Hz; 7d, (24.39±0.36) Hz, $P<0.001$) for corresponding background periods in CCW command generation. Thus, 7b more strictly obeyed the triple-step threshold algorithm than 7d during WD periods of T5, suggesting a flexible role of 7d in generating more STOP commands to maintain water access, and more CW rotation commands to counteract CCW movement. During this WD period of T5, overall, STOP commands were the most frequent, while CW commands were the least

frequent (in %; STOP, 43.33; CCW, 34.83; CW, 21.84).

During NWD periods of T5, activities of neurons 7b and 7d also showed similar trends for command generation as in the WD periods. However, in contrast to WD periods, both neurons exhibited distinctively different firing rates for each of three commands (in Hz, Neuron 7b: CW, 35.74±1.45; CCW, 18.47±0.75; STOP, 23.93±0.53; CW vs. CCW, $P<0.001$; CCW vs. STOP, $P<0.001$; CW vs. STOP, $P<0.001$; Neuron 7d: CW, 18.58±0.82; CCW, 33.20±1.02; STOP, 22.38±0.43; CW vs. CCW, $P<0.001$; CCW vs. STOP, $P<0.001$; CW vs. STOP, $P<0.05$). In addition, both neurons also showed significantly different background firing rates for the period of 301 to 500 ms prior to and 500 ms after generation of each of three commands (in Hz, Neuron 7b: CW, 25.54±0.30; CCW, 23.53±0.21; STOP, 23.61±0.20; Neuron 7d: CW, 24.47±0.31; CCW, 25.78±0.22; STOP, 24.87±0.23; 7b vs. 7d: CW, $P<0.05$; CCW, $P<0.001$; STOP, $P<0.01$). Thus, during NWD peri-

ods, both neurons strictly followed the triple-step threshold algorithm more closely than during WD periods of T5. During the NWD period of T5, overall, STOP commands were the most frequent and CW commands were the least frequent (in %, STOP, 40.23; CCW, 37.19; CW, 22.58).

During the 6 min of T5, there were 29 WD and 30 NWD periods. Wheel movements in two WD and three NWD periods are shown in Figure 2D. In this example, WD-1 consisted of several repetitions of two different modes of water drinking, i.e., water drinking while issuing CCW wheel rotations (WD-CCWs) and water drinking during fine control (WD-FCs) of wheel rotations while generating combinations of three commands. During WD-CCWs, the water-containing region of the rotating wheel moved towards the rat at the beginning of the WD-1 period and moved away from the rat at the later period of the WD-1. During WD-FCs, the wheel movements were maintained around a fixed position because of many STOP commands and antagonistic actions between CW and CCW commands. In contrast to the WD-1 period, the WD-2 period involved many WD-FCs; the WD-1 period contained 23 CCWs, seven CWs and 30 STOPs, while the WD-2 period contained four CCWs, four CWs and 13 STOPs. The relative predominance of CCWs over CWs commands during the WD-1 period is demonstrated by the finding that mean firing rate of 7d ((29.79 ± 1.92) Hz, i.e., threshold value 3 for CCW) was significantly (P=0.0186) higher than that of 7b ((23.51 ± 1.79) Hz, i.e., threshold value 2 for CW, Figure 2E). During the WD-2 period, the mean activity of 7b ((31.47 ± 2.53) Hz, i.e., threshold value 3 for CW) was similar to that of 7d ((30.59 ± 3.45) Hz, i.e., threshold value 3 for CCW), ensuring more frequent generation of STOP (i.e., CCW 3–CW 3=0) commands.

As indicated above, two units (7b and 7d) were directly responsible for command generation. Throughout T1–T5, units 7b and 7d showed strong positive correlations ((r)>0.6) during WD periods (Figure 2F and G), but were not significantly correlated during NWD periods (Figure 2H and I). Another 12 neurons simultaneously recorded close to 7b and 7d were also involved, either directly or indirectly, in command generation. These neurons were differentially related to activity changes of either 7b or 7d during the WD and NWD periods (Figure 2F–I, Table 1). In general, unit 7d (Figure 2G–I) exhibited a higher positive correlations to other neurons compared to unit 7b (Figure 2F–H), regardless of WD or NWD period. Thus, these results suggest that highly correlated influences from other neurons might be required for the flexible role of unit 7b in generating appropriate commands to enable water access during WD periods. Eight units (5c, 5d, 6b, 6c, 7a, 7c, 8b, and 8c) showed strong correlations ((r)>0.6) with unit 7d during WD periods throughout five trials, but only three units (6c, 7c, and 8b) exhibited strong correlations during NWD periods (Table 1). None of the 12 units showed any correlation with

unit 7b during WD period of T1, but eight units (5c, 6a, 6b, 6c, 7a, 7c, 8a, and 8b) exhibited strong relations during the WD period of T2. During the WD period of T3 and T5, all units except unit 5a exhibited strong correlations with 7b. During T4, all units, except 5a and 5d, exhibited strong correlations with unit 7b. Thus, from T2 to T5, six units (5c, 6b, 6c, 7a, 7c, and 8b) exhibited strong correlations with both 7b and 7d during WD periods. However, unit 5a was not correlated to either neuron regardless of WD or NWD period. Units 5d and 8c exhibited more preferential correlations with unit 7d than unit 7b during WD periods of T1–T5, whereas units 5b, 6a, and 8a showed a preference for unit 7b over unit 7d. Thus, units 5d and 8c might preferentially modulate unit 7d's activity in generating threshold values of either CCW 0 or CCW 1. In addition, units 5b, 6a, and 8a might be preferentially involved in flexible control of unit 7b's activity to generate threshold values of either CW 0 or CW 3. However, these preferential influences on 7b and 7d appeared to be indirect, since cross-correlation analyses did not reveal any immediate (presumably synaptic) modulations. During NWD periods throughout T1–T5, unit 7b was not correlated with most other simultaneously recorded units, except for three units (5c, 6b, and 8a) at T5. Three other units (5a, 5b, and 6a) were related to neither 7b nor 7d units during NWD periods throughout T1–T5.

Other simultaneously recorded neurons' activities at T5 were also analyzed to test whether they had any correlation with either unit 7b or 7d during the 200 ms prior to each command generation (Table 2). During the overall WD period of T5, neither 7b nor 7d exhibited a significant correlation with other simultaneously recorded neurons. However, 7b and 7d exhibited negative relation ((r)=−0.61) to each other prior to CW command generation and mild relation (but significant, (r)=−0.54) between them prior to CCW command generation during WD periods of T5. During NWD periods of T5, much stronger negative correlations between two units were found prior to CCW generation ((r)=−0.88) than prior to CW output ((r)= −0.62). Unit 6c exhibited a strong positive correlation with unit 7d, and a negative correlation with unit 7b during the NWD period. These correlation analyses coincided with CCW dominance (i.e., threshold value 3 for CCW) during the NWD period and the importance of CW movements (i.e., threshold value 3 for CW) during the WD period. Units 7b and 7d did not exhibit any significant correlations between them prior to generating STOP commands during both WD ((r)=−0.1076) and NWD ((r)= −0.0414) periods of T5. This was natural, since the threshold value for CW 0 was generated consistently by the different mean firing rates of 7b during the WD and NWD periods. Threshold values for CW 0 and CW 1 were determined by the lack of a significant difference between 7d's mean firing rates responsible for the two commands (as stated earlier) during the WD period.

The results indicated that a trial-dependent increase of

Table 1   Correlations between control signals in 7b and 7d and signals in other cells[a]

Ref	7d	5a	5b	5c	5d	6a	6b	6c	7a	7b	7c	8a	8b	8c
	T5	0.57	0.67*	0.80*	0.74*	0.74*	0.82*	0.89*	0.80*	0.75*	0.84*	0.74*	0.83*	0.80*
	T4	0.53	0.54	0.77*	0.84*	0.45	0.84*	0.92*	0.75*	0.61*	0.86*	0.56	0.83*	0.68*
WD	T3	0.57	0.73*	0.80*	0.83*	0.76*	0.89*	0.93*	0.82*	0.74*	0.91*	0.67*	0.88*	0.74*
	T2	0.53	0.05	0.65*	0.80*	0.75*	0.94*	0.90*	0.79*	0.77*	0.89*	0.75*	0.82*	0.60*
	T1	0.57	0.43	0.82*	0.78*	0.66*	0.82*	0.87*	0.90*	0.70*	0.88*	0.58	0.82*	0.76*

Ref	7b	5a	5b	5c	5d	6a	6b	6c	7a	7b	7d	8a	8b	8c
	T5	0.57	0.71*	0.81*	0.65*	0.78*	0.82*	0.77*	0.76*	0.76*	0.75*	0.83*	0.74*	0.76*
	T4	0.55	0.72*	0.71*	0.48	0.76*	0.77*	0.60*	0.64*	0.60*	0.61*	0.77*	0.68*	0.70*
WD	T3	0.43	0.81*	0.83	0.61*	0.80*	0.89*	0.82*	0.71*	0.76*	0.74*	0.72*	0.72*	0.90*
	T2	0.45	0.17	0.68*	0.58	0.81*	0.75	0.80*	0.64*	0.67*	0.77*	0.78*	0.74*	0.53
	T1	0.37	0.16	0.41	0.35	0.47	0.52	0.42	0.44	0.48	0.57	0.34	0.37	0.52

Ref	7d	5a	5b	5c	5d	6a	6b	6c	7a	7b	7c	8a	8b	8c
	T5	0.27	0.40	0.61*	0.65*	0.56	0.68*	0.82*	0.66*	0.49	0.77*	0.50	0.72*	0.63*
	T4	0.23	0.22	0.60*	0.64*	0.44	0.57	0.81*	0.58	0.26	0.76*	0.09	0.60*	0.56
NWD	T3	0.39	0.27	0.60*	0.59	0.38	0.61*	0.80*	0.61*	0.33	0.75*	0.17	0.71*	0.45
	T2	0.07	−0.12	0.34	0.42	0.27	0.60*	0.79*	0.52	0.09	0.72*	0.12	0.65*	0.38
	T1	0.49	0.09	0.50	0.71*	0.46	0.62*	0.85*	0.74*	0.29	0.80*	0.20	0.75*	0.44

Ref	7b	5a	5b	5c	5d	6a	6b	6c	7a	7b	7d	8a	8b	8c
	T5	0.34	0.57	0.63*	0.36	0.58	0.70*	0.55	0.50	0.54	0.49	0.65*	0.54	0.62*
	T4	0.20	0.38	0.36	0.08	0.41	0.44	0.25	0.27	0.25	0.26	0.28	0.28	0.26
NWD	T3	0.24	0.39	0.43	0.00	0.36	0.56	0.28	0.33	0.26	0.33	0.52	0.37	0.45
	T2	0.01	−0.01	0.12	−0.12	0.21	0.32	0.12	0.07	0.08	0.09	0.19	0.09	0.17
	T1	0.20	0.19	0.37	0.09	0.40	0.55	0.28	0.28	0.26	0.29	0.42	0.26	0.42

a) *, $P<0.05$.

Table 2   Neuronal activities 200 ms prior to STOP, CCW, and CW commands were correlated to Ref 7b and 7d during WD and NWD[a]

	WD	5a	5b	5c	5d	6a	6b	6c	7a	7b	7c	7d	8a	8b	8c
STOP	Ref 7b	−0.11	0.29	−0.14	−0.12	0.10	0.30	−0.27	0.20		−0.30	−0.11	−0.07	0.02	−0.06
	Ref 7d	−0.44	−0.22	0.23	−0.27	−0.07	−0.12	−0.44	−0.48	−0.11	−0.24		0.06	−0.14	0.16
CCW	Ref 7b	0.22	0.19	0.16	0.01	0.18	−0.28	−0.10	−0.24		0.00	−0.54*	0.24	−0.41	−0.24
	Ref 7d	−0.14	0.05	0.25	0.45	−0.07	0.31	0.30	0.00	−0.54*	0.11		−0.01	0.34	0.49
CW	Ref 7b	0.31	0.27	0.32	0.22	0.09	0.33	−0.01	0.15		−0.13	−0.61*	0.30	0.32	0.22
	Ref 7d	−0.30	−0.12	−0.31	−0.28	−0.39	−0.01	0.28	−0.24	−0.61*	−0.14		−0.17	−0.04	−0.36
	WD	5a	5b	5c	5d	6a	6b	6c	7a	7b	7c	7d	8a	8b	8c
STOP	Ref 7b	−0.32	0.12	−0.05	0.30	0.15	0.36	0.20	−0.18		0.05	−0.04	0.02	0.40	−0.21
	Ref 7d	−0.21	−0.05	0.06	−0.24	−0.16	0.41	0.07	−0.25	−0.04	−0.02		0.23	−0.25	0.12
CCW	Ref 7b	−0.21	0.19	−0.29	−0.33	0.12	−0.33	−0.64*	0.21		−0.51	−0.88*	−0.09	−0.31	−0.05
	Ref 7d	0.04	−0.22	0.36	0.39	−0.09	0.32	0.64*	−0.11	−0.88*	0.25		0.14	0.43	−0.06
CW	Ref 7b	−0.07	0.33	−0.13	−0.07	0.20	0.21	−0.08	0.29		−0.10	−0.62*	0.40	−0.07	0.29
	Ref 7d	0.28	−0.25	0.16	0.12	−0.11	−0.06	0.34	−0.43	−0.62*	−0.02		−0.14	0.25	0.05

a) *, $P<0.05$.

total water drinking duration (TWD duration) (%) was strongly ((r)=0.9053) correlated with the change in WD frequency (Figure 3A). This trial-dependent WD frequency augmentation was predominantly related to the change of CW ((r)=0.9920) movement, and average water drinking duration (AWD duration) was highly related to the occurrence of STOP commands ((r)=0.9419; Figure 3B). If water dish control using the BCI system to quench thirstiness was motivational, the proportion of the generation of the three commands might be different among various behavioral states. During the 6 min sleep period, in which rats did not have any motivation to drink water and presumably no motivation to control the BCI system, CW commands were rare, while STOP commands were numerous (Figure 3C). During WD periods of T5, CW commands were dominant, whereas CCW were the least prevalent. However, during NWD periods of T5 (T-NWD), CW and CCW were observed in similar proportions. Command proportions during the NWD periods were quite similar to those when water dish control was allowed but water access was blocked by placing the water dish far away from the rat (FAR in Figure 3C). This result might be expected, since rats were moti-
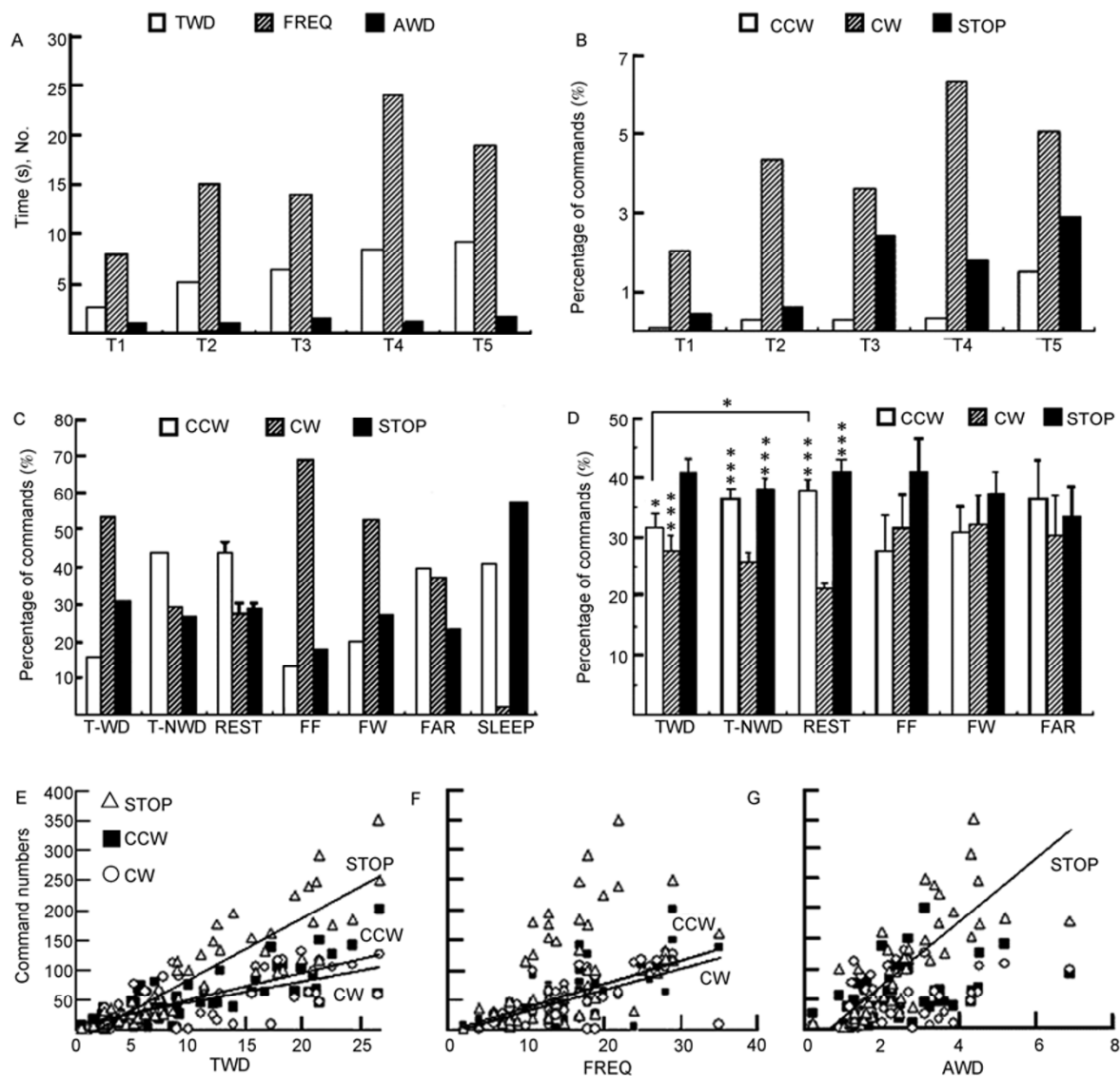
Figure 3 A, Histogram showing total WD, frequency, and AWD in five trials. B, Histogram of CCW, CW, and STOP commands in different trials. C, Histogram of distribution of three commands in different sessions. D, Statistical comparison of CCW, CW, and STOP commands in different sessions of 16 rats. *, $P<0.05$; **, $P<0.01$; ***, $P<0.001$. E–G, Correlations of CW, CCW, and STOP commands with TWD, frequency, and AWD.

vated to control the BCI system during the T-NWD and FAR periods, but experienced difficulty accessing the water dish. During six repetitions of the resting (REST) periods between five trial periods, rats had to wait 6 min to start new WD trial since the chamber was blocked by paper, and thereby would be expected to give up the motivation of controlling the BCI system. CCW commands were most frequently observed in this period. Proportions of the three commands generated when the rat was allowed free access to water (FW) by fixing the water dish in front of the rat were similar to those in the T-WD condition. However, the frequencies of CW and CCW were different between the two behavioral states. The proportions of the three commands generated when the rat had free access to food (FF; by placing food pellets in the rat chamber) were similar to

those in the T-WD condition. However, the frequencies of CCW and STOP commands were different between the two behavioral states. Overall, the proportions of command generation during the T-WD, FF, and FW periods indicated that CW commands occurred commonly, whereas the T-NWD, REST, and FAR periods were associated with more frequent CCW commands. Averaged proportions of the generation of the three commands from 16 rats during various behavioral states (T-WD, $n=59$; T-NWD, $n=59$; REST, $n=102$; FF, $n=14$; FW, $n=14$; FAR, $n=4$) are shown in Figure 3D. During T-WD, STOP commands were significantly more numerous than either CW or CCW commands. However, during both T-NWD and REST periods, CW commands were significantly fewer than either CCW or STOP commands. In addition, CCW occurrence during
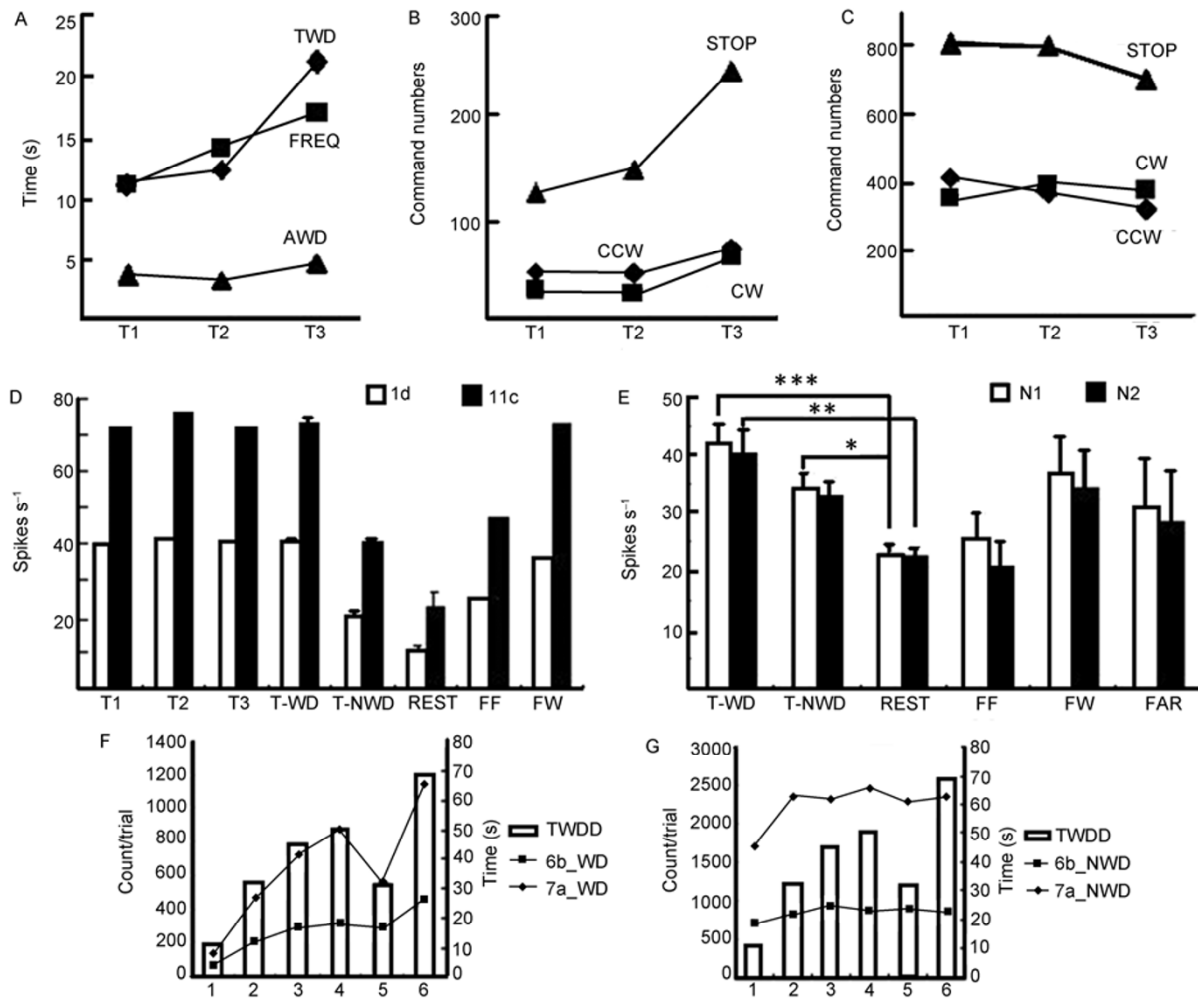
Figure 4   A, TWD, frequency, and AWD changes in the first three trials. B, Change in CCW, CW, and STOP commands in the first three trials during WD. C, Change in CCW, CW, and STOP commands in the first three trials during NWD. D, Activities of two controlling neurons in different sessions. E, Statistical analysis of neuronal activity in different sessions. *, $P<0.05$; **, $P<0.01$; ***, $P<0.001$. F and G, Burst analysis. Maximum interval to start burst, 0.02 s; maximum interval to end burst, 0.02 s; minimum interval between bursts, 0.02 s; minimum duration of burst, 0.08 s; minimum number of spikes in burst, 4. F, WD period; G, non-WD period.

REST was significantly more frequent than during T-WD. Averaged proportions of three command generations were similar during the FF, FW, and FAR periods. During REST, CW occurrence was significantly less frequent than during either the T-NWD or FW periods. The relationships between BCI efficiency (TWD, FREQ, and AWD) and three commands generated during T-WDs from 56 trials in 16 rats were analyzed (Figure 3E–G). TWD changes from trial to trial exhibited linear correlations with all three commands (CCW, $(r)=0.7696$; CW, $(r)=0.6596$), and were most strongly correlated with the STOP command $((r)=0.8980)$. WD frequency was linearly related to both CCW $((r)=0.6982)$ and CW $((r)=0.6732)$ commands. AWD duration was significantly correlated with the STOP command $((r)=0.7922)$.

The experimental results revealed that TWD (%) and WD frequency were increased from T1 to T3 (Figure 4A).

During T-WD periods, the frequency of STOP $((r)=0.9970)$ commands was related to TWD changes (Figure 4B). At T3, the frequency of all three commands was increased. During T-NWD periods, both STOP and CCW commands decreased in frequency from T1 to T3. In addition, neurons 1d and 11c were set to encode CCW and CW commands, respectively (Figure 3D). Triple-step thresholds for unit 1d were set to 30, 20, 10 in Hz (CCW threshold values: above 30: 3, 20–29: 2, 10–19: 1, below 19: 0) and those of 11c were to 60, 40, and 20 in Hz (CW threshold values: above 40: 3, 40–39: 2, 20–39: 1, below 20: 0). Firing rates of both 1d and 11c were above each neuron's threshold level 3 during T-WD periods from T1 to T3. During T-NWD periods, the activities of both 1d and 11c were a range that could generate each neuron's threshold value of either 2 or 1. During resting periods, both neurons' firings were at levels for generating threshold values of either 1 or 0. Average
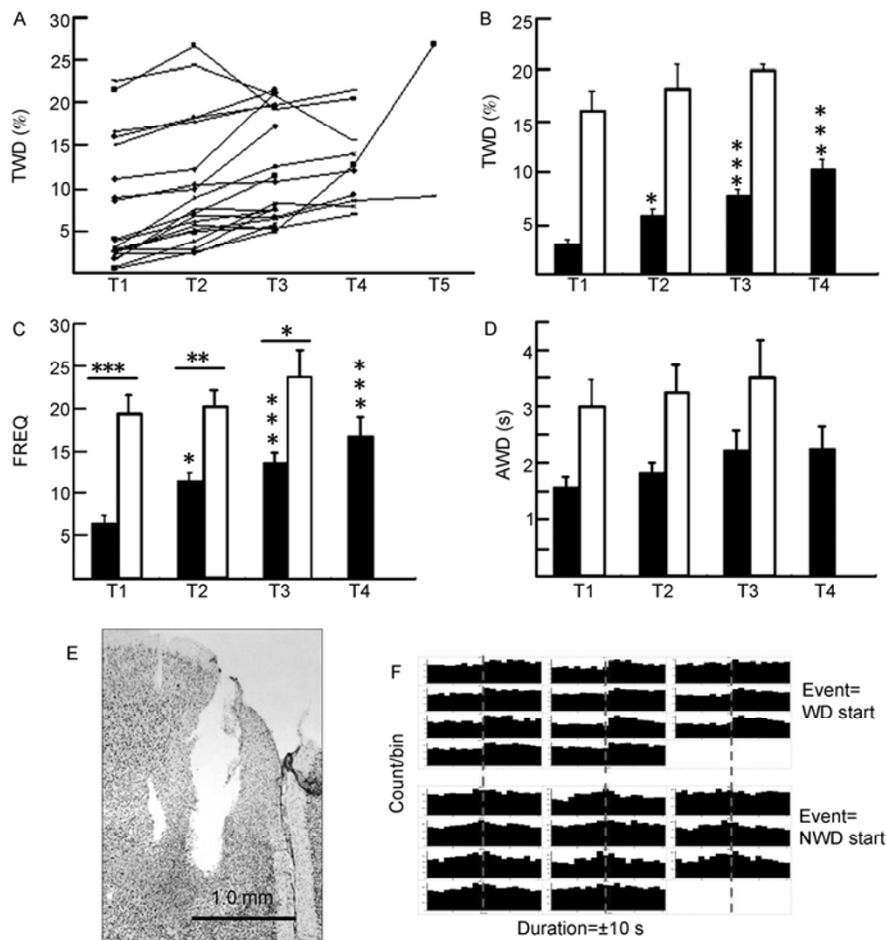
Figure 5   A, Percentage of TWD in all experiments. B−D, Change of TWD, frequency, and AWD in all experiments in the first four trials. *, $P<0.05$; **, $P<0.01$; ***, $P<0.001$. E, Histology of implantation site in the PFC (cresyl violet stain). F, Perievent histogram of 11 signals. The dotted line shows the initial of WD (above) and NWD (below).

activity of 1d during rest was significantly lower than during T-NWD ($P=0.0024$) and during T-WD ($P=0.0238$). Average activity of 11c during rest was also significantly lower from that during T-NWD ($P=0.0238$) and that during T-WD ($P<0.0001$). Activity of 1d and 11c during FW period was similar to that during the T-WD period. Activity of both neurons during FF was similar to those during the T-NWD period. Averaged activities of N1s and N2s from 16 rats during the resting period were significantly lower than during either T-WD or T-NWD (Figure 4E). In another case, the number of firing bursts exhibited by neuron 6b and 7a in WD and NWD was compared in Figure 4F and G. A significant correlation ($P=0.0018$ for 6b, $P<0.0001$ for 7a) was found between neuronal bursting and duration of WD, but this was not found for NWD ($P=0.2125$ for 6b, $P=0.0782$ for 7a).

In Figure 5, trial-dependent BCI efficiency changes obtained from 16 rats were examined in terms of % TWD duration, frequency of WD and AWD duration per trial. TWD (%) at T1 was found to be variable, ranging from 0.56% to 21.54% in the 6 min period (Figure 5A). Thirteen of 20 rats

showed trial-dependent gradual increases of BCI efficiency measured by TWD and WD frequency (Figure 5B and C). Most of these rats showed less than 5% TWD at T1. The seven rats not showing trial-dependent BCI efficiency increases tended to exhibit higher TWD (8.96%−22.67%), even at T1. Averaged WD durations per trial did not change as trials were repeated. Thus, BCI efficiency augmentation occurred when initial efficiency was quite low. This mainly occurred with the increment of WD frequency. The WD amount was measured after each trial, and averaged WD amount per second was (0.049±0.010) mL. Figure 5F shows neuronal activity pre- and post-WD, with a bin size of 1 s. Neuronal activity significantly increased in WD compared to pre-WD ($P<0.01$), and post-WD neuron activity gradually decreased in the 10 s period after WD.

3   Discussion

Teuber [25] hypothesized that PFC neurons play a vital role in processing signals from sensory to motor information.

Here, we found that PFC neurons could function as an adaptive goal-encoding region to fulfill an animal's requirements when spontaneous signals were transformed in real-time through a simple BCI system into commands for controlling a machine. The current study produced the following major findings: (i) Using a simple algorithm, we found that rats were able to control a BCI system using the activity of single neurons in PFC. (ii) PFC neurons provided a feasible adaptive choice for animals to manipulate a machine after learning in several training sessions. (iii) Motivational control of our BCI system was evidenced by differential changes of neuronal activity with experience, and the appropriate generation of three commands during various behavioral states, such as resting, free food, free water, and FAR periods.

A closed loop information stream was constructed in the design of a BCI system: This loop involved a thirsty rat with a motivation to drink, a triple-threshold algorithm (Figure 1) to convert neural signals into machine control commands, and a command execution system. This loop was completed when the rat began to notice and understand the function of the reward system. To investigate whether rats could be trained (i.e., could encode the necessary information) to comprehend the relation between their mental state and the movement of the dish, they were required to accomplish the task of controlling a water-provision system that rotated in 1-D. A trial-dependent BCI efficiency increase was observed. This increase was particularly apparent when initial efficiency at trial 1 was very low (Figure 5). However, when initial efficiency was high above 10% of 6 min, rats tended to show less motivation to control the BCI system after three trials. Intentional differences were also expressed in the proportions of the three generated commands. In the sleep period there was presumably no motivation to drink water, and thereby no motivation to control the BCI system. The proportions of three commands generated during this sleep period were markedly different from those during WD trial periods (Figure 3C). During the 6 min resting periods between the trial periods, the rat had to wait for the next trial, holding the motivation of WD. Although this is a short interval, the rat also had to wait for the next T-WD period during the T-NWD periods between the T-WD periods. This similarity was reflected in the proportions of three commands between the T-NWD and the resting periods (Figure 3C and D). For trained rats, the rotating dish served as a visual cue. The NWD periods effectively constituted 'delay' durations in the task. This might explain the persistence of neuronal activity that resulted in different proportions of commands from the resting and FAR sessions [26]. During the FAR period, the rat was able to watch the water dish movement with the motivation to drink water, but was unable to access the water for 6 min. Command generation during FW was largely similar to those in T-WD, even though there was no actual control of the water dish movement during this period. Command generation during FF

(Figure 3C) was similar to that during FW, but CW was further increased while CCW and STOP commands were decreased. This similarity may reflect the common motivation to fulfill its appetite, while the difference may be related to the absence of motivational control of the water dish, since food pellets were given freely in the chamber, rather than on the controllable water dish. The proportion of the three commands generated during the FF, FW, FAR periods was quite variable among 16 rats, but did not significantly differ between rats (Figure 3D). This suggests that the necessity of strict regulation of command generation was commonly absent, compared to during WD trials.

In the current study, maximum BCI efficiency was lower than 30%, and was increased by the elevation of WD frequency. If we suppose that the system was rotated in one direction with a specified angle for a trial without a STOP command, the rat was able to access the water dish for 86º. In this case, the efficiency would be 23.9%, and one cycle of rotation took 3.35 s for three steps (21.5°), and 4.97 s for one step (14.5°) of angular movement. Thus, the estimated averaged WD duration ranged from 0.80 to 1.19 s, and WD frequency ranged from 72.5 to 107.5 times for 6 min of a trial period. The overall averaged WD duration was (2.37±0.17) s for whole trials (*n*=56), and the averaged WD frequency was (15.09±0.99) times for a trial period (the highest WD frequency was 35). These findings indicate that actual BCI control was not performed by simple rotation in one direction (Figure 3F), and that water drinking was not performed by chance during wheel rotation. The occurrence of STOP commands during the fine control period aided the increase in average WD duration (Figure 3G), but most strongly decreased the WD frequency during the non-WD period of a trial. One of the counter actions for the two directional commands was appropriate in the fine control period and for the WD frequency increase (Figure 3F). However, dominant command generation for one direction during the non-WD period served to speed up the next period of access to water (Figure 3D). The lowest performance of the current BCI system could be achieved by fixing or moving the water dish to a position that was not accessible by the rat. This non-accessible region covers 72.1% of the wheel rotation. On the other hand, the best performance in our BCI system could be achieved by moving the water containing region, while issuing a 1:1 ratio of CW and CCW commands, and many STOP commands (Figure 3G), directly in front of the rat; the water-containing region covered 23.9% of the wheel rotation. This type of optimal performance is shown as WD-FC during the WD-2 period in Figure 2D.

Compared with decoding algorithms, encoding algorithms require fewer signals (minimum of two), to reach high efficiency, which in return could perform a greater number of functions using a similar number of neurons in decoding. Accordingly, this algorithm causes less damage than methods requiring massive implantation of brain tissue.

The remarkable cortical plasticity of the brain means that signals from implanted electrodes can, after adaptation, be utilized by electrodes and computers [27]. Because PFC neurons perform various functions, such as prediction, working memory and discrimination, the mean, maximum, and minimum frequency of PFC neurons in a rat, or among different rats, was not consistent. The average spontaneous firing rate of the population of neurons was (5.9±1.6) (SD) spikes s^{-1}. Although each neuron's absolute activity level was important for the generation of a normalized threshold value, the difference between two normalized threshold values (N1 and N2) encoded from two neurons' activities was the factor determining which of the three commands was given (CW: 3, 2, 1; CCW: −3, −2, −1; STOP: 0). This algorithm meant that two neurons could fire in a negatively correlated fashion, even though the two neurons were recorded from a single wire, for the generation of CW and CCW commands, and in an uncorrelated fashion for the STOP command during the 200 ms pre-command period (Figure 2A and B, Table 2). The effectiveness of this triple threshold comparator algorithm was predominantly restricted to the designated N1 and N2 neurons, although there were many neurons in the vicinity of the two neurons (Table 2). This result may partially reflect that the PFC is not construed simply as a cluster of neurons, but as a network [28].

The trial-dependent BCI efficiency increase was largely due to the increase in WD frequency (Figure 5C), since average WD duration was not significantly altered over subsequent trials (Figure 5D). However, the activities of N1 and N2 during the resting period, when the rat sat in the chamber for 6 min without seeing the water dish (i.e., without the visual cue) and therefore with no motivation to control the BCI system, were significantly lower than those during the T-WD trial period (Figure 4D and E) [29]. The comparison of the number of neuronal bursts in WD with NWD further supports this notion (Figure 4F and G). A number of previous studies have reported that neuronal units exhibit accelerating discharge during delay periods while animals prepare for movement in a variety of tasks, including delay tasks [28,30–33]. In the current study, neuronal activity during T-NWD was intermediate between T-WD and resting periods. Both neurons exhibited elevated activity during motivational control of the water dish, and suppressed activity during resting periods. This finding indicates that STOP commands observed during T-WD period and the resting period were generated by distinct levels of similar threshold values dictated by two neurons.

1   Lucas J W, Schiller J S, Benson V. Summary health statistics for U.S. adults: national health interview survey. Vital Health Stat, 2004, 10: 60–62

2   Hochberg L R, Serruya M D, Friehs G M, *et al*. Neuronal ensemble control of prosthetic devices by a human with tetraplegia. Nature, 2006, 442: 164–171

3   Felton E A, Garell P C, Williams J C, *et al*. Electrocorticographically controlled brain-computer interfaces using motor and sensory imagery in patients with temporary subdural electrode implants. Report of four cases. J Neurosurg, 2007, 106: 495–500

4   Fabiani G E, McFarland D J, Pfurtscheller G, *et al*. Conversion of EEG activity into cursor movement by a brain-computer interface (BCI). IEEE Trans Neural Syst Rehabil Eng, 2005, 12: 331–339

5   Cincotti F, Mattia D, Aloise F, *et al*. Non-invasive brain-computer interface system: towards its application as assistive technology. Brain Res Bull, 2008, 75: 796–803

6   Bai O, Lin P, Vorbach S, *et al*. A high performance sensorimotor beta rhythm-based brain-computer interface associated with human natural motor behavior. J Neural Eng, 2008, 5: 24–35

7   Velliste M, Perel S, Spalding M C, *et al*. Cortical control of a prosthetic arm for self-feeding. Nature, 2008, 453: 1098–1101

8   Moritz C T, Perlmutter S I, Fetz E E. Direct control of paralysed muscles by cortical neurons. Nature, 2008, 456: 639–642

9   Kennedy P R, Andreasen D, Ehirim P, *et al*. Using human extra-cortical local field potentials to control a switch. J Neural Eng, 2004, 1: 72–79

10   Serruya M D, Hatsopoulos N G, Paninski L, *et al*. Instant neural control of a movement signal. Nature, 2002, 416: 141–142

11   Taylor D M, Tillery S I, Schwartz A B. Direct cortical control of 3d neuroprosthetic devices. Science, 2002, 296: 1829–1832

12   Carmena J M, Lebedev M A, Crist R E. Learning to control a brain-machine interface for reaching and grasping by primates. PLoS Biol, 2003, 1: e42

13   Shenoy K V, Meeker D, Cao S, *et al*. Neural prosthetic control signals from plan activity. Neuroreport, 2003, 14: 591–596

14   Musallam S, Corneil B D, Greger B, *et al*. Cognitive control signals for neural prosthetics. Science, 2004, 305: 258–262

15   Olson B P, Si J, Hu J, *et al*. Closed-loop cortical control of direction using support vector machines. IEEE Trans Neural Syst Rehabil Eng, 2005, 13: 72–80

16   Wessberg J, Stambaugh C R, Kralik J D, *et al*. Real-time prediction of hand trajectory by ensembles of cortical neurons in primates. Nature, 2000, 408: 361–365

17   Carmena J M, Lebedev M A, Crist R E, *et al*. Learning to control a brain–machine interface for reaching and grasping by primates. PLoS Biol, 2003, 1: 193–208

18   Serruya M D, Hatsopoulos N G, Paninski L, *et al*. Instant neural control of a movement signal. Nature, 2002, 416: 141–142

19   Fuster J M. The Prefrontal Cortex, 2nd ed. New York: Raven Press, 1989

20   Salzman C D, Fusi S. Emotion, cognition, and mental state representation in amygdala and prefrontal cortex. Annu Rev Neurosci, 2010, 33: 173–202

21   Paxinos G, Watson C. The Rat Brain in Stererotaxic coordinates, 4th ed. San Diego: Academic Press, 1999. 96–101

22   Yoshio S, Susumu T. Dynamic synchrony of firing in the monkey prefrontal cortex during working-memory tasks. J Neurosci, 2006, 26: 10141–10153

23   In K H, Ki Y Y, Hua L, *et al*. Indole-3-propionic acid attenuates neuronal damage and oxidative stress in the ischemic hippocampus. J Neurosci Res, 2009, 87: 2126–2137

24   Chapin J K, Moxon K A, Markowitz R S, *et al*. Real-time control of a robot arm using simultaneously recorded neurons in the motor cortex. Nat Neurosci, 1999, 2: 664–670

25 Teuber H L. Unity and diversity of frontal lobe functions. Acta Neurobiol Exp(Wars), 1972, 32: 615–656

26 Fuster J M. Unit activity in prefrontal cortex during delayed-response performance: neuronal correlates of transient memory. J Neurophysiol, 1973, 36: 61–78

27 Levine S P, Huggins J E, BeMent S L, *et al*. A direct brain interface based on event-related potentials. IEEE Trans Rehabil Eng, 2000, 8: 180–185

28 Fuster J M, Bauer R H, Jervey J P. Cellular discharge in the dorsolateral prefrontal cortex of the monkey in cognitive tasks. Exp Neurol, 1982, 77: 679–694

29 Fuster J M, Jervey J P. Neuronal firing in the inferotemporal cortex of the monkey in a visual memory task. J Neurosci, 1982, 2: 361–375

30 Kubota K, Iwamoto T, Suzuki H. Visuokinetic activities of primate prefrontal neurons during delayed-response performance. J Neurophysiol, 1974, 37: 1197–1212

31 Sakai M. Prefrontal unit activity during visually guided lever pressing reaction in the monkey. Brain Res, 1974, 81: 297–309

32 Niki H, Watanabe M. Prefrontal unit activity and delayed response: relation to cue location versus direction of response. Brain Res, 1976, 105: 79–88

33 Boch R A, Goldberg M E. Participation of prefrontal neurons in the preparation of visually guided eye movements in the rhesus monkey. J Neurophysiol, 1989, 61: 1064–1084